NATIONAL ADVISORY COMMITTEE FOR AERONAUTICS

TECHNICAL MEMORANDUM 1415

LAMINAR FLOW ABOUT A ROTATING BODY OF REVOLUTION IN AN AXIAL AIRSTREAM

By H. Schlichting

Translation of "Die laminare Strömung um einen axial angeströmten rotierenden Drehkörper." Ingenieur-Archiv, vol. XXI, no. 4, 1953.

Washington
February 1956

NATIONAL ADVISORY COMMITTEE FOR AERONAUTICS

TECHNICAL MEMORANDUM 1415

LAMINAR FLOW ABOUT A ROTATING BODY OF REVOLUTION IN AN AXIAL AIRSTREAM*

By H. Schlichting

1. INTRODUCTION

The flow about a body of revolution rotating about its axis and simultaneously subjected to an airstream in the direction of the axis of rotation is of importance for the ballistics of projectiles with spin. In jet engines of all kinds, too, an important role is played by the flow phenomena on a body which is situated in a flow and which at the same time performs a rotary motion. Investigations of C. Wieselsberger[1] regarding the air drag of slender bodies of revolution which rotate about their axis and are at the same time subjected to a flow in the direction of the axis of rotation showed a considerable increase of the drag with the ratio of the circumferential velocity to the free-stream velocity - increasing more and more, the slenderer the body. Similar results were obtained by S. Luthander and A. Rydberg[2] in tests on rotating spheres which are subjected to a flow in the direction of the axis of rotation. These authors observed, in particular, a considerable shifting of the critical Reynolds number of the sphere dependent on the ratio of the circumferential velocity to the free-stream velocity. The physical reason for these phenomena may be found in the processes in the friction layer where, due to the rotary motion, the fluid corotates in the neighborhood of the wall and, consequently, is subjected to the influence of a strong centrifugal force. It is clear that the process of separation and also the transition from laminar to turbulent conditions are strongly affected thereby, and that, therefore, the rotary motion must exert a strong influence on the drag of the body.

---

*"Die laminare Strömung um einen axial angeströmten rotierenden Drehkörper." Ingenieur-Archiv, vol. XXI, no. 4, 1953, pp. 227-244.- An abstract from this report was read on the VIII International Mechanics Congress in Istanbul on August 27, 1952.

[1]C. Wieselsberger, Phys. Z. 28, 1927, p. 84.

[2]S. Luthander, A. Rydberg, Phys. Z. 36, 1935, p. 552.

In the flow processes in the corotating layer of the fluid, one deals with complicated three-dimensional boundary-layer flows which so far have been little investigated, experimentally as well as theoretically. Th. v. Kármán[3] treated at an early date the special case of a disk rotating in a stationary liquid, for laminar and turbulent flow, as a boundary-layer problem, according to an approximation method. Later, W. G. Cochran[4] also solved this problem for the laminar case as an exact solution of the Navier-Stokes equations. A generalization of this case, namely the flow about a rotating disk in a flow approaching in the direction of the axis of rotation, for laminar flow, has been treated recently by H. Schlichting and E. Truckenbrodt[5]. The result most important for practical purposes are the formulas for the torque of the rotating disk; it is highly dependent on the ratio of the circumferential velocity to the free-stream velocity of the disk.

For the general case of a rotating body simultaneously subjected to a flow, J. M. Burgers[6] gave a few general formulations. We have set ourselves the problem of calculating the laminar flow on a body of revolution in an axial flow which simultaneously rotates about its axis[7]. The problem mentioned above, the flow about a rotating disk in a flow, which we solved some time ago, represents the first step in the calculation of the flow on the rotating body of revolution in a flow insofar as, in the case of a round nose, a small region about the front stagnation point of the body of revolution may be replaced by its tangential plane.

In our problem regarding the rotating body of revolution in a flow, for laminar flow, one of the limiting cases is known: that of the body which is in an axial approach flow but does not rotate. The solution of

---

[3]Th. v. Kármán, Z. angew. Math. Mech. 1, 1921, p. 235.

[4]W. G. Cochran, Proc. Cambridge Philos. Soc. 30, 1934, p. 365.

[5]H. Schlichting, E. Truckenbrodt, Z. angew. Math. Mech. 32, 1952, p. 97; abstract in Journal Aeron. Sciences 18, 1951, p. 638.

[6]J. M. Burgers, Kon. Akad. van Wetenschappen, Amsterdam 45, 1941, p. 13.

[7]It is pointed out that the turbulent case, for the rotating disk in a flow as well as for the rotating body of revolution in a flow, meanwhile has been solved, in continuation of the present investigations, by E. Truckenbrodt. Publication will take place later.- E. Truckenbrodt, "Die Strömung an einer angeblasenen rotierenden Scheibe bei turbulenter Strömung," will be published in Z. angew. Math. Mech.- E. Truckenbrodt "Ein Quadraturverfahren zur Berechnung der Reibungsschicht an axial angeströmten rotierenden Drehkörpern." Report 52/20 of the Institut für Strömungsmechanik der T. H. Braunschweig, 1952.

this case was given by S. Tomotika[8], by means of transfer of the well known approximation method of K. Pohlhausen[9] to the rotationally symmetrical case. The other limiting case, namely the flow in the neighborhood of a body which rotates but is not subjected to a flow is known only for the rotating circular cylinder[10], aside from the rotating disk. In the case of the cylinder one deals with a distribution of the circumferential velocity according to the law $v = \omega R^2/r$ where R signifies the cylinder radius, r the distance from the center, and ω the angular velocity of the rotation. The velocity distribution as it is produced here by the friction effect is therefore the same as in the neighborhood of a potential vortex. In contrast to the first limiting case (nonrotating body subjected to a flow), the flow in the case of slender bodies which rotate about their longitudinal axis in a stationary fluid does not have "boundary-layer character," that is, the friction effect is not limited to a thin layer in the proximity of the wall but takes effect in the entire environment of the rotating body.

Very recently, L. Howarth[11] also made an attempt at solution for a sphere rotating in a stationary fluid. This flow is of such a type that in the friction layer the fluid is transported by the centrifugal forces from the poles to the equator, and in the equator plane flows off toward the outside.

When we treat, in what follows, the general case of the rotating body of revolution in a flow according to the calculation methods of Prandtl's boundary-layer theory, we must keep in mind that this solution cannot contain the limiting case of the body of revolution which only rotates but is not subjected to a flow. However, this is no essential limitation since this case is not of particular importance for practical purposes.

The dominant dimensionless quantity for our problem is the ratio

$$\frac{\text{Circumferential velocity}}{\text{Free-stream velocity}} = \frac{V_m}{U_\infty} = \frac{R_m\omega}{U_\infty}$$

where R_m is to denote the radius of the maximum cross section of the body of revolution. The calculations must aim at determining for a prescribed body of revolution the torque, the drag, and beyond that, the entire boundary-layer variation as a function of V_m/U_∞. The

---

[8]S. Tomotika, "Laminar Boundary Layer on the Surface of a Sphere in a Uniform Stream." ARC Rep. 1678, 1935.

[9]K. Pohlhausen, Z. angew. Math. Mech. 1, 1921, p. 253.

[10]H. Schlichting, "Grenzschicht-Theorie," p. 63. Karlsruhe 1951.

[11]L. Howarth, Philos. Mag. VII Ser. 42, 1951, p. 1,308.

particular case $V_m/U_\infty = 0$ is already known from the boundary-layer theory established so far. Considering what has been said above, we must not expect our solution to be valid for arbitrarily large V_m/U_∞. The upper limit of the value of V_m/U_∞ for which our calculations holds true, still remains to be determined. Presumably, it will lie considerably above $V_m/U_\infty = 1$.

2. THE FUNDAMENTAL EQUATIONS

We take the coordinate system indicated in figure 1 as a basis for the calculation of the flow. Let (x,y,z) be a rectangular curvilinear fixed coordinate system. Let the x-axis be measured along a meridional section, and the y-axis along a circular cross section so that the xy-plane is the tangential plane. The z-axis is at right angles to the tangential plane. Let u, v, w be the velocity components in the direction of these three coordinate axes. Furthermore, let R(x) be the radius of the circular cross section, ω the angular velocity of rotation, U(x) the potential-theoretical velocity distribution, and $\nu = \mu/\rho$ the kinematic viscosity.

The equations of motion simplified according to the calculation methods of the boundary-layer theory are for this coordinate system

$$\frac{\partial u}{\partial x} + \frac{u}{R}\frac{dR}{dx} + \frac{\partial w}{\partial z} = 0 \qquad \text{(continuity)} \qquad (1)$$

$$u\frac{\partial u}{\partial x} - \frac{v^2}{R}\frac{dR}{dx} + w\frac{\partial u}{\partial z} = U\frac{dU}{dx} + \nu\frac{\partial^2 u}{\partial z^2} \qquad \text{(momentum, meridional)} \qquad (2)$$

$$u\frac{\partial v}{\partial x} + \frac{uv}{R}\frac{dR}{dx} + w\frac{\partial v}{\partial z} = \nu\frac{\partial^2 v}{\partial z^2} \qquad \text{(momentum, azimuthal)} \qquad (3)$$

The boundary conditions are

$$z = 0: \quad u = 0, \quad v = v_0 = R\omega, \quad w = 0; \quad z = \infty: \quad u = U(x), \quad v = 0 \qquad (4)$$

A solution of this system of differential equations for an arbitrarily prescribed body shape $R(x)$ with the pertaining potential theoretical velocity distribution $U(x)$ leads to insurmountable mathematical difficulties. We use therefore the more convenient approximation method which makes use of the momentum theorem. We obtain the two momentum equations for the meridional and the azimuthal direction by integration of the corresponding equations of motion over z from the wall $z = 0$ to a distance $z = h > \delta$ which lies outside of the friction layer.

For the meridional direction there results by integration of (2) over z, with consideration of the continuity equation (1) and after introduction of the wall-shear stress for the x-direction

$$\tau_{x_0} = \mu\left(\frac{\partial u}{\partial z}\right)_0 \tag{5}$$

the momentum equation for the meridional direction

$$U^2\frac{d\vartheta_x}{dx} + U\frac{dU}{dx}\left(2\vartheta_x + \delta_x^*\right) + \frac{1}{R}\frac{dR}{dx}\left(U^2\vartheta_x + v_0^2\vartheta_y\right) = \frac{\tau_{x_0}}{\rho} \tag{6}$$

Therein, as is well known,

$$\delta_x^* = \int_0^\delta \left(1 - \frac{u}{U}\right)dz \tag{7}$$

is the displacement thickness whereas

$$\vartheta_x = \int_0^\delta \frac{u}{U}\left(1 - \frac{u}{U}\right)dz \tag{8}$$

$$\vartheta_y = \int_0^\delta \left(\frac{v}{v_0}\right)^2 dz \tag{9}$$

may be denoted as momentum-loss thicknesses for the x- or y-direction.

In an analogous manner there results for the azimuthal direction by integration of (3) over z with consideration of the continuity equation (1) and introduction of the wall-shear stress for the y-direction

$$\tau_{y_0} = \mu\left(\frac{\partial v}{\partial z}\right)_0 \tag{10}$$

as the momentum theorem for the circumferential direction

$$\omega\frac{d}{dx}\left(UR^3\vartheta_{xy}\right) = -R^2\frac{\tau_{y_0}}{\rho} \tag{11}$$

Therein

$$\vartheta_{xy} = \int_0^\delta \frac{u}{U}\frac{v}{v_0}dz \tag{12}$$

has been introduced as the "momentum loss thickness due to spin."

3. APPROXIMATION METHODS

(a) The Velocity Distributions

According to the approximation method of the boundary-layer theory as given first by Th. v. Kármán and K. Pohlhausen, the momentum equations (6) and (11) are satisfied by setting up suitable formulations for the velocity distributions u and v which satisfy the most important boundary conditions. For the present case, two parameters may still be left undetermined in these equations for the determination of which the two momentum equations are then available. As expressions for the velocity distribution, polynomials in the distance from the wall have proved to be suitable, with the property that the boundary layer joins at a finite wall distance $z = \delta$ the frictionless outer flow. The boundary-layer thickness may be different for the meridional and the azimuthal velocity component. Let these boundary-layer thicknesses be δ_x and δ_y, respectively; we introduce the dimensionless wall distances formed with them

$$\frac{z}{\delta_x} = t \quad \text{and} \quad \frac{z}{\delta_y} = t' \tag{13}$$

For the velocity distributions u and v, we select polynomials of the fourth degree in t and t', respectively. These contain five coefficients each so that, for determination of these coefficients, we can satisfy five boundary conditions each for u and v. We choose the following 10 boundary conditions:

$$\left.\begin{aligned} &t = 0: \quad u = 0 && \nu\frac{\partial^2 u}{\partial z^2} = -U\frac{dU}{dx} - \frac{v_0^2}{R}\frac{dR}{dx} \\ &t = 1: \quad u = U && \frac{\partial u}{\partial z} = 0 \qquad \frac{\partial^2 u}{\partial z^2} = 0 \end{aligned}\right\} \quad (14a,b,c,d,e)$$

$$\left.\begin{aligned} &t' = 0: \quad v = v_0 = R\omega && \frac{\partial^2 v}{\partial z^2} = 0 \\ &t' = 1: \quad v = 0 && \frac{\partial v}{\partial z} = 0 \qquad \frac{\partial^2 v}{\partial z^2} = 0 \end{aligned}\right\} \quad (15a,b,c,d,e)$$

The boundary conditions (14a, b, c) and (15a, b, c) result immediately from the fundamental equations (2) and (3) with (4) for $z = 0$ and $z = \delta_x$ or δ_y. The remaining boundary conditions provide a gentle transition of the boundary layer into the outer flow. Taking these boundary conditions into consideration, one obtains the following polynomials as expressions for the velocity distributions

$$\frac{u}{U} = 2t - 2t^3 + t^4 + K\frac{1}{6}\left(t - 3t^2 + 3t^3 - t^4\right) \tag{16}$$

$$\frac{v}{v_0} = 1 - 2t' + 2t'^3 - t'^4 \tag{17}$$

Therein

$$K = \frac{\delta_x^2}{\nu}\left[\frac{dU}{dx} + \left(\frac{v_0}{U}\right)^2 \frac{U}{R}\frac{dR}{dx}\right] \tag{18}$$

is a form parameter of the u-velocity profile, which is analogous to the form parameter λ of the Pohlhausen method[12]. The velocity distributions u/U and v/v_0 are represented in figure 2.

Let the point of separation be given by the beginning of the return flow of the meridional velocity component $u(z)$ in the proximity of the wall

$$\left(\frac{\partial u}{\partial z}\right)_{z=0} = 0$$

This yields

$$K = -12 \text{ (separation)} \tag{19}$$

The expression for the u-component is the same as in the Pohlhausen method for the plane and rotationally symmetrical case. This guarantees that our solution in the case without rotation, $\omega = 0$, will be transformed into the solution of S. Tomotika and F. W. Scholkemeyer[13] for the nonrotating body of revolution. Introduction of the expressions (16) and (17) into the momentum equations (6) and (11) yields two differential equations for the still unknown boundary-layer thicknesses $\delta_x(x)$ and $\delta_y(x)$ or the quantities derived from them.

(b) The Momentum Equation for the Circumferential Direction

We present first the further calculation for the momentum equation of the circumferential direction. With

$$\frac{\tau_{y_0}}{\rho} = \nu\left(\frac{\partial v}{\partial z}\right)_0 = -2\frac{\nu}{\delta_y}R\omega \tag{20}$$

there results from (11), after division by ω,

$$\frac{d}{dx}\left\{R^3 U \vartheta_{xy}\right\} = 2\frac{\nu}{\delta_y}R^3 \tag{21}$$

---

[12]Cf. H. Schlichting, "Grenzschicht-Theorie," p. 193.

[13]F. W. Scholkemeyer, "Die laminare Reibungsschicht an rotationssymmetrischen Körpern." Dissertation Braunschweig 1943, Cf. H. Schlichting, Grenzschicht-Theorie, p. 204.

With introduction of the further parameters

$$g_0 = \frac{\vartheta_{xy}}{\delta_y} \quad \text{and} \quad \Delta = \frac{\delta_y}{\delta_x} \tag{22}$$

as well as

$$\Theta = \frac{\vartheta_{xy}^2}{\nu} \tag{23}$$

and

$$\sigma = \Theta\left(\frac{dU}{dx} + 3\frac{U}{R}\frac{dR}{dx}\right) \tag{24}$$

one obtains from (21) the following differential equation for $\Theta(x)$

$$\frac{d\Theta}{dx} = \frac{G(K,\Delta)}{U} \tag{25}$$

Therein is

$$G(K,\Delta) = 4g_0 - 2\sigma \tag{26}$$

a universal function of the two parameters K and Δ.

This function has been determined already by W. Dienemann[14] in the calculation of the temperature boundary layer on a cylinder (two-dimensional problem).[15] For the temperature distribution in the boundary layer there we chose the same polynomial of the fourth degree as we did for the azimuthal velocity distribution according to (17). According to (12) we have

$$g_0 = \frac{\vartheta_{xy}}{\delta_y} = \int_0^1 \frac{u}{U}\frac{v}{v_0}dt'$$

Because of

$$t = \frac{z}{\delta_x} = \frac{z}{\delta_y}\frac{\delta_y}{\delta_x} = t'\Delta$$

---

[14]W. Dienemann, "Berechnung des Wärmeüberganges an laminar umströmten Körpern mit konstanter und ortsveränderlicher Wandtemperatur." Dissertation Braunschweig, 1951, Z. angew. Math. Mech. 33, 1953, p. 89.

[15]With the symbols according to W. Dienemann there apply the identities $H_t \equiv g_0$ and $\Lambda \equiv K$.

one obtains after calculation of the integral with the velocity distributions (16) and (17) the quantity g_0 as a function of K and Δ. According to W. Dienemann, there results

$$g_0(K,\Delta) = g_1(\Delta) + Kg_2(\Delta) \tag{27}$$

$$\left.\begin{aligned}
\Delta \leqq 1: \quad g_1(\Delta) &= \frac{2}{15}\Delta - \frac{3}{140}\Delta^3 + \frac{1}{180}\Delta^4 \\
g_2(\Delta) &= \frac{1}{90}\Delta - \frac{1}{84}\Delta^2 + \frac{3}{560}\Delta^3 - \frac{1}{1,080}\Delta^4 \\
\Delta \geqq 1: \quad g_1(\Delta) &= \frac{3}{10} - \frac{3}{10}\frac{1}{\Delta} + \frac{2}{15}\frac{1}{\Delta^2} - \frac{3}{140}\frac{1}{\Delta^4} + \frac{1}{180}\frac{1}{\Delta^5} \\
g_2(\Delta) &= \frac{1}{120}\frac{1}{\Delta} - \frac{1}{180}\frac{1}{\Delta^2} + \frac{1}{840}\frac{1}{\Delta^4} - \frac{1}{3,024}\frac{1}{\Delta^5}
\end{aligned}\right\} \tag{28}$$

The function $g_0(\Delta)$ as a function of Δ for various values of K is represented in figure 3. Table 1 gives a few numerical values of the functions $g_1(\Delta)$ and $g_2(\Delta)$.

TABLE I.- THE UNIVERSAL FUNCTIONS $g_1(\Delta)$ AND $g_2(\Delta)$ ACCORDING TO EQUATION (28)

Δ	$g_1(\Delta)$	$100g_2(\Delta)$
0	0	0
.2	.0053	.036
.4	.0208	.114
.6	.0457	.205
.7	.0606	.249
.8	.0784	.291
.9	.0970	.329
1.0	.1175	.364
1.2	.1614	.423
1.4	.2089	.471
1.6	.2589	.510
1.8	.3109	.541
2.0	.3643	.568
2.5	.5021	.618
3.0	.6437	.651

(c) The Momentum Equation for the Meridional Direction

Further transformation of the momentum equation for the meridional direction yields, if one introduces, according to Holstein-Bohlen[16] and analogous to (23)

$$Z = \frac{\vartheta_x^2}{\nu} \qquad \chi = Z\frac{dU}{dx} \tag{29}$$

the following differential equation for $Z(x)$

$$\frac{dZ}{dx} = \frac{F(K,\Delta)}{U} \tag{30}$$

Therein

$$F(K,\Delta) = 2\left\{f_3 - (2\chi + \chi f_2) - Z\frac{U}{R}\frac{dR}{dx}\left[1 + \left(\frac{v_0}{U}\right)^2 \frac{h_0\Delta}{f_0}\right]\right\} \tag{31}$$

exactly as $G(K,\Delta)$ in (26) a universal function of the two parameters K and Δ. Individually, the following relationships apply:

$$f_0(K) = \frac{\vartheta_x}{\delta_x} = \frac{37}{315} - \frac{K}{945} - \frac{K^2}{9{,}072} \tag{32}$$

$$f_1(K) = \frac{\delta_x^*}{\delta_x} = \frac{3}{10} - \frac{K}{120} \tag{33}$$

$$f_2(K) = \frac{\delta_x^*}{\vartheta_x} = \frac{f_1(K)}{f_0(K)} \tag{34}$$

$$\frac{\Delta}{f_0(K)} = \frac{\delta_y}{\delta_x}\frac{\delta_x}{\vartheta_x} = \frac{\delta_y}{\vartheta_x} \tag{35}$$

$$f_3(K) = \frac{\tau_{x_0}}{\mu}\frac{\vartheta_x}{U} = \left(\frac{\partial u}{\partial z}\right)_0 \frac{\delta_x}{U}\frac{\vartheta_x}{\delta_x} = \left(2 + \frac{K}{6}\right)f_0(K) \tag{36}$$

[16]Cf. H. Schlichting, Grenzschicht-Theorie, p. 195.

$$h_0 = \frac{\vartheta_y}{\delta_y} = \frac{23}{126} \tag{37}$$

The above functions of K are already known from the calculation of the boundary layer of the two-dimensional case.[17]

The connection between Z and K results from (18), with consideration of (29) and (32), and is

$$Kf_0^2(K) = Z\left[\frac{dU}{dx} + \left(\frac{v_0}{U}\right)^2 \frac{U}{R}\frac{dR}{dx}\right] \tag{38}$$

Taking $\chi = ZU'$, from (29), into consideration, one may write this because of (32) also in the form

$$\chi\left[1 + \left(\frac{v_0}{U}\right)^2 \frac{U}{R}\frac{R'}{U'}\right] = \chi^* = K\left(\frac{37}{315} - \frac{K}{945} - \frac{K^2}{9,072}\right)^2 \tag{39}$$

In figure 4 the universal functions f_0, f_2, f_3, and K are represented as functions of χ^*. At the point of separation, for arbitrary rotational velocity, one will have, because of $K = -12$, the parameter $\chi^* = -0.1567$. At the stagnation point, without rotation, $K = 4.716$ and $\chi^* = 0.05708$, whereas with rotation the values at the stagnation point are dependent on the spin parameter v_0/U (cf. the following section). From (38) the form parameter K can be determined when Z is given. Furthermore, for the later calculation a connection between the parameters Δ, g_0, Θ, Z, and K is needed. There results according to (22), (23), (29), and (32) as follows

$$\Delta g_0(K,\Delta) = \sqrt{\frac{\Theta}{Z}}\, f_0(K) \tag{40}$$

The two differential equations (25) for $\Theta(x)$ and (30) for $Z(x)$ are two simultaneous differential equations coupled by the universal functions $G(k,\Delta)$ and $F(K,\Delta)$. In the case of the nonrotating body, $v_0 = 0$, the coupling is eliminated since then, according to (31), the function F becomes independent of Δ and remains dependent only on K.

---

[17]Cf. H. Schlichting, Grenzschicht-Theorie, Chapter XII.

In this case, one can first determine $Z(x)$ from (30), and subsequently $\Theta(x)$ from (25). This solution for Θ has - it is true - no physical significance. It serves merely for giving the limiting value for vanishing speed of rotation.

(d) The Initial Values at the Stagnation Point

At the stagnation point where $U = 0$, the two differential equations (25) and (30) have a singular value since in both equations on the right side the denominator vanishes. In order to obtain at the stagnation point initial slopes of finite magnitude, $d\Theta/dx$ and dZ/dx finite, the numerators also must disappear in these two equations for the stagnation point. This requirement yields the initial values of the parameters K_0 and Δ_0 at the stagnation point. For the potential flow there applies at the stagnation point

$$x \longrightarrow 0: \quad U(x) = U_0'R = aR \qquad \frac{dR}{dx} = 1 \tag{41}$$

The initial values of the meridional equation are obtained from $F = 0$ according to (31)

$$f_{30} - 2\chi_0 - \chi_0 f_{20} - \chi_0\left[1 + \frac{h_0}{f_{00}}\Delta_0\left(\frac{\omega}{a}\right)^2\right] = 0$$

With

$$K_0 f_{00}^2 = \chi_0\left[1 + \left(\frac{\omega}{a}\right)^2\right]$$

according to (38), with

$$f_{30} = f_{00}\left(2 + \frac{K_0}{6}\right)$$

according to (36), and h_0 according to (37), there results after a brief calculation

$$\frac{K_0}{1 + \left(\frac{\omega}{a}\right)^2} = \frac{2 + \left(\frac{1}{6} - \frac{23}{126}\Delta_0\right)K_0}{\frac{137}{210} - \frac{29}{2{,}520}K_0 - \frac{1}{3{,}024}K_0^2 - \frac{23}{126}\Delta_0} \tag{42}$$

For a given speed of rotation ω/a, this is the first equation between the initial values K_0 and Δ_0. For the case without rotation, $\omega = 0$, the boundary-layer thickness ratio Δ_0 drops out from this equation, and an equation for the initial value K_0 only remains which reads

$$2 + \frac{51}{105}K_0 + \frac{29}{2,530}K_0^2 + \frac{1}{3,024}K_0^3 = 0 \tag{43}$$

The physically useful solution of this equation is

$$\left(K_0\right)_{\omega=0} = K_{00} = 4.716 \tag{44}$$

as known according to S. Tomotika.

For the initial values of the azimuthal equation, one obtains from $G = 0$ according to (26)

$$2g_0\left(K_0,\Delta_0\right) - \sigma\left(K_0,\Delta_0\right) = 0$$

Because of

$$\sigma\left(K_0,\Delta_0\right) = 4a\Theta_0 = 4ag_{00}^2\Delta_0^2\frac{\delta_{x_0}^2}{\nu}$$

according to (24) and

$$K_0 = \frac{a\delta_{x_0}^2}{\nu}\left[1 + \left(\frac{\omega}{a}\right)^2\right]$$

according to (18) and because of (27) one obtains after a short intermediate calculation

$$\frac{K_0}{1 + \left(\frac{\omega}{a}\right)^2} = \frac{1}{2\left[g_1(\Delta_0) + K_0 g_2(\Delta_0)\right]\Delta_0^2} \tag{45}$$

For a given speed of rotation ω/a, this is the second equation between the initial values K_0 and Δ_0.

For the case without rotation, $\omega = 0$, one obtains from (45) with $K_0 = K_{00} = 4.716$ according to (44) for the initial value of $\left(\Delta_0\right)_{\omega=0} = \Delta_{00}$ the equation

$$1 - 9.432\Delta_{00}^2\left[g_1\left(\Delta_{00}\right) + 4.716 g_2\left(\Delta_{00}\right)\right] = 0 \tag{46}$$

Hence results with $g_1(\Delta)$ and $g_2(\Delta)$ according to (27) and (28)

$$\Delta_{00} = 0.915 \tag{47}$$

The ratio of the boundary-layer thicknesses $\Delta = \delta_y/\delta_x$ for the azimuthal and meridional velocity distribution therefore lies near 1 which is physically plausible.

The two equations (42) and (45) now represent, for prescribed angular velocity ω/a, two equations for the initial values K_0 and Δ_0. A solution was obtained by determining from both equations the values of $K_0\Big/\left[1 + \left(\frac{\omega}{a}\right)^2\right]$ as a function of Δ_0 for various fixed values K_0. Hence, the initial values indicated in table 2 result. These values are presented in figure 5 as a function of ω/a. It was found that for values of $\omega/a > 0.815$, no usable initial values of K_0 and Δ_0 exist; that is, our method fails for these larger values of ω/a. The limit beyond which our calculation method fails coincides with the value $K = 12$ of the form parameter[18]. The initial values χ_0, χ_0^*, and g_{00} determined from the initial values K_0 and Δ_0 are represented in figure 5 and table 2, as a function of ω/a.

[18]For $K > 12$, because of the effect of the centrifugal forces, it is entirely possible in the present case to obtain velocity profiles with $u/U > 1$.

TABLE 2.- INITIAL VALUES AT THE STAGNATION POINT

$\frac{\omega}{a}$	K_0	Δ_0	$100\chi_0$	$100\chi_0^*$	$\frac{1}{2}g_{00}$
0	4.716	0.915	5.71	5.71	0.0629
.221	5	.908	5.71	5.99	.0632
.454	6	.882	5.70	6.89	.0640
.679	8	.838	5.69	8.32	.0651
.785	10	.781	5.69	9.19	.0661
.815	12	.726	5.69	9.49	.0664

Finally we obtain the initial value for Z simply in the following manner with $U_0' = a$

$$Z_0 = \frac{\chi_0}{a} \tag{48}$$

The initial value for Θ results with $\sigma_0 = 2g_{00}$ according to (24) as

$$\Theta_0 = \frac{1}{2}\frac{g_{00}}{a} \tag{49}$$

The expression for the velocity distribution used here (parabola of the fourth degree for u and v) is different from that of our former calculation[19] for the rotating disk in a flow. It must be expected, however, that the boundary-layer parameters of the rotating disk in a flow should agree approximately with those at the stagnation point of the rotating body of revolution if both methods are to yield usable results. We give this comparison for the momentum-loss thickness in x-direction (8) at the stagnation point and for the meridional component of the wall shear stress at the stagnation point. The dimensionless momentum-loss thickness at the stagnation point is according to (29) with $U_{x=0}' = a$

$$\vartheta_{x_0}\sqrt{\frac{a}{\nu}} = \sqrt{\chi_0} \tag{50}$$

[19]See footnote 5 on page 2.

The meridional component of the wall-shear stress at the stagnation point $\left(\tau_{x_0}\right)_{x=0} = \tau_{r_0}$ is according to (5), (16), and (32)

$$\frac{\tau_{r_0}}{\rho U^2}\sqrt{\frac{UR}{\nu}} = \sqrt{\frac{\nu}{a}}\,\frac{f_0(K_0)}{\vartheta_{x_0}}\left[2 + \frac{1}{6}K_0\right] \tag{51}$$

The values calculated accordingly are compared with those of the rotating disk in figure 6.[20] The agreement up to the validity limit of our calculation ($\omega/a = 0.815$) is quite satisfactory.

Hence we conclude that our present calculation yields satisfactory results in the entire range $0 \leq \omega/a \leq 0.815$.

4. TORQUE AND FRICTIONAL DRAG

(a) Torque

The entire torque of the body of revolution may be easily ascertained from the results of the boundary-layer calculation in the following manner: The contribution of an element of the body of revolution with the radius $R(x)$ and the arc length dx is (fig. 7)

$$dM = -2\pi R^2 \tau_{y_0} dx$$

and thus the total torque

$$M = -2\pi \int_0^{x_A} \tau_{y_0} R^2 dx \tag{52}$$

where x_A signifies the arc length from the stagnation point to the point of separation. Taking the momentum theorem for the circumferential direction (11) into consideration, one obtains

---

[20] Whereas the values for the wall-shear stress could be taken directly from the report referred to in footnote 5 (p. 227, table 2), the values for the momentum-loss thickness were calculated subsequently with application of equation (8) with the velocity distributions indicated there.

$$M = 2\pi\rho\omega\left[R^3 U \vartheta_{xy}\right]_0^{x_A} = 2\pi\rho R_A{}^3 U_A \vartheta_{xy_A} \tag{53}$$

where the subscript A denotes the values at the separation point. From the boundary-layer calculation, one knows the value of the momentum thickness due to spin at the separation point in the dimensionless form

$$\frac{\vartheta_{xy_A}}{R_m}\sqrt{\frac{U_\infty R_m}{\nu}} = B \tag{54}$$

where R_m is assumed to denote the radius of the maximum cross-sectional area.

If one introduces - in the same manner as for the rotating disk - a dimensionless spin coefficient by

$$c_M = \frac{M}{\frac{\rho}{2}\omega^2 R_m{}^5} \tag{55}$$

one obtains

$$\frac{V_m}{U_\infty}\sqrt{\frac{U_\infty R_m}{\nu}}c_M = 4\pi B\left(\frac{R_A}{R_m}\right)^3\frac{U_A}{U_\infty} \tag{56}$$

where $V_m = R_m\omega$ is the circumferential velocity of the maximum cross-sectional area. Since, as the completely calculated examples show, the dimensionless momentum thickness due to spin B varies at the separation point only a little with V_m/U_∞, c_M is in first approximation proportional to U_∞/V_m and inversely proportional to the Reynolds number $\sqrt{U_\infty R_m/\nu}$.

For the case of the rotating disk in a flow, with the radius $R_m = R$, one obtains because of $R_A = R$, $U_A = aR$ from (56) in combination with (54)

$$\sqrt{\frac{R^2\omega}{\nu}}\,c_M = 4\pi\vartheta_{xy}\sqrt{\frac{a}{\nu}}\sqrt{\frac{a}{\omega}} \tag{57}$$

and with the numerical value

$$\sqrt{\frac{a}{\nu}}\,\vartheta_{xy} = \left(\sqrt{\frac{g_{00}}{2}}\right)_{\omega/a=0} = 0.251$$

according to (49)

$$\sqrt{\frac{R^2\omega}{\nu}}\,c_M = 3.15\sqrt{\frac{a}{\omega}}$$

in very good agreement with the former investigation[21] where the numerical value is 3.17.

(b) Frictional Drag

The frictional drag of the rotating body of revolution may be determined by integration of the wall-shear stress components τ_{x_0}. A surface ring element of the body of revolution with the radius $R(x)$ and the arc length dx (fig. 7) yields the drag

$$dW = 2\pi R\tau_{x_0}d\bar{x} \tag{58}$$

Therein $\bar{x}$ is the coordinate measured along the body axis. Integration from the stagnation point $x = 0$ to the separation point $\bar{x}_A$, where $\tau_{x_0} = 0$, yields

$$W = 2\pi\int_0^{\bar{x}_A} \tau_{x_0}R\,d\bar{x} \tag{59}$$

We shall refer the drag to the maximum cross-sectional area πR_m^2 and define the drag coefficient

$$c_w = \frac{W}{\frac{\rho}{2}U_\infty^2\pi R_m^2} \tag{60}$$

---

[21]Cf. footnote 5 on page 2, equation (49a).

Since we obtain the wall-shear stress in the dimensionless form

$$\frac{\tau_{x_0}}{\rho U_\infty^2}\sqrt{\frac{U_\infty R_m}{\nu}} = T \tag{61}$$

we may write for the drag coefficient

$$\sqrt{\frac{U_\infty R_m}{\nu}}\, c_w = 4\int_0^{\bar{x}_A/R_m} T\frac{R}{R_m}\, d\frac{\bar{x}}{R_m} \tag{62}$$

5. EXAMPLES

(a) Sphere

As the first example, the friction layer on the rotating sphere was calculated. When R_m signifies the sphere radius, x the arc length, and $x/R_m = \varphi$ the center angle measured starting from the stagnation point, the radius distribution is

$$R(x) = R_m \sin \varphi \tag{63}$$

and the theoretical potential velocity distribution

$$U(x) = \frac{3}{2}U_\infty \sin \varphi \tag{64}$$

The velocity gradient at the stagnation point is

$$a = \left(\frac{dU}{dx}\right)_{x=0} = \frac{3}{2}\frac{U_\infty}{R_m}$$

and thus

$$\left(\frac{V_m}{U_\infty}\right)_0 = \frac{\omega R_m}{U_\infty} = \frac{3}{2}\frac{\omega}{a} \tag{65}$$

Since, according to the explanations in section 3, the calculation can be carried out only for $\omega/a \leqq 0.815$, we must limit ourselves to $V_m/U_\infty \leqq \frac{3}{2} 0.815 = 1.22$.

The solutions are obtained by numerical integration of the two simultaneous differential equations (25) and (30) for the two cases $V_m/U_\infty = 0$ and 1. The calculation scheme is given in table 3. The results for further values of V_m/U_∞ could hence be obtained conveniently by interpolation. The case $V_m/U_\infty = 0$ (nonrotating sphere) agrees with the case of Scholkemeyer[22]. The results of the calculation are represented in table 4 and figures 8 to 12.

TABLE 3.- CALCULATION SCHEME FOR THE SOLUTION OF THE TWO SIMULTANEOUS DIFFERENTIAL EQUATIONS (25) AND (30)

ω prescribed							Z_ν	x	x*	K	f_0	f_2	f_3
φ	x	R(x)	$\frac{dR}{dx} = R'$	U(x)	$\frac{dU}{dx} = U'$	$v_0 = \omega R$							
							Initial value given (eq. (48))	=ZU'	Eq. (39)	Fig. 4 initial value (table 2)	Fig. 4	Fig. 4	Fig. 4
Given body form and potential flow							To be calculated line by line						

Θ_ν	2σ	$g_0\Delta$	Δ	$4g_0$	$\left(\frac{v_0}{U}\right)^2 \frac{h_0\Delta}{f_0}$	F	$\frac{dZ}{dx}$	ΔZ	$Z_{\nu+1}$	G	$\frac{d\Theta}{dx}$	$\Delta\Theta$	$\Theta_{\nu+1}$
Initial value (eq. (49))	Eq. (24)	Eq. (40)	Fig. 3	$4\frac{g_0\Delta}{\Delta}$	$h_0 = \frac{23}{126}$	Eq. (31)	Eq. (30)			Eq. (26)	Eq. (25)		
To be calculated line by line													

TABLE 4.- POSITION OF SEPARATION POINT AND OF THE TORQUE IN DEPENDENCE ON V_m U_∞ FOR THE ROTATING SPHERE IN A FLOW

Spin parameter, $\frac{V_m}{U_\infty}$	Separation point, $\varphi_A{}^o$	Torque, $\frac{V_m}{U_\infty}\sqrt{\frac{U_\infty R_m}{\nu}}\, c_M$
0	108.2	9.15
.25	108.0	9.14
.50	107.3	9.06
.75	106.2	9.03
1.00	104.9	8.95
1.22	103.5	8.85

[22]Footnote 13 on page 8.

Figure 8 gives the variation of the form parameter K of the meridional component of the velocity distribution in the boundary layer. The initial values K_0 at the stagnation point are immediately given in table 2 with equation (65). At maximum velocity, $\varphi = 90^\circ$, K is, according to (18), equal to zero for all V_m/U_∞, because in a sphere at the point where $dU/dx = 0$, also $dR/dx = 0$. The value $K = -12$ gives the position of the separation point A. In figure 8 the variation of the boundary-layer thickness ratio $\Delta = \delta_y/\delta_x$ is also plotted; it always lies close to 1 and also changes only little with V_m/U_∞. Figure 9 shows the variation of the momentum thickness due to spin ϑ_{xy}. The curves for various V_m/U_∞ almost coincide. The same is true for the momentum-loss thickness ϑ_x and the friction-layer thicknesses δ_x and δ_y. Figure 10 shows the variation of the meridional and azimuthal component of the wall-shear stress. The meridional component τ_{x_0} increases with the spin coefficient V_m/U_∞ only a little whereas the azimuthal component τ_{y_0} in first approximation is proportional to the spin coefficient V_m/U_∞. The position of the separation point as a function of the spin coefficient V_m/U_∞ is given in table 4. For the nonrotating sphere $\varphi_A = 108.2^\circ$, and for $V_m/U_\infty = 1.22$ the separation point shifts forward to $\varphi_A = 103.5^\circ$. This displacement of the separation point because of the rotation is due to the effect of the centrifugal forces and is, clearly, immediately plausible. For the velocity profiles behind the equatorial plane ($\varphi > 90^\circ$), the centrifugal forces have the effect of an additional pressure increase in flow direction and therefore cause the separation point to shift forward. In figure 11 the dimensionless torque coefficient formed according to equation (56) is represented as a function of the spin coefficient V_m/U_∞. (Cf. table 4.) One sees that the proportionality with V_m/U_∞ is fulfilled with very good approximation. Finally, figure 12 shows several velocity profiles in photographic reproduction.

A sphere is rather unsuitable for the comparison of the theoretical calculation with test results, because of the large dead-water zone which has the effect that even in the case of the nonrotating sphere the positions of the separation point according to theory and to measurement do not agree when the boundary-layer calculation is based on the potential-theoretical pressure distribution as we have done here. A valid comparison regarding the influence of the rotation on the behavior of the friction layer can be made only for a slender body where no noteworthy dead-water zone develops. Nevertheless we mention here the measured results of S. Luthander and A. Rydberg [23]. In figure 13 the drag coefficient of the sphere in dependence on the Reynolds number Re for various values of V_m/U_∞ is given according to these measurements. For the nonrotating sphere, $V_m/U_\infty = 0$, and up to values of V_m/U_∞ to about 3, the curve c_w against Re shows the characteristic variation with

[23] Footnote 2 on page 1.

the familiar sudden drop at the so-called critical Reynolds number. It is known that for Reynolds numbers below the critical Reynolds number the friction layer undergoes laminar separation, and for numbers above the critical Reynolds number, in contrast, a turbulent one. In the case without rotation, the laminar separation point lies at about $\varphi = 81^\circ$, the turbulent one, in contrast, at about $\varphi = 110^\circ$ to 120°. The measurements with rotation show for $V_m/U_\infty = 0$ to 1.4 a shifting of the critical Reynolds numbers toward higher values of Re. This shifting of the critical Reynolds number to higher values for small V_m/U_∞ is probably brought about by the fact that for $V_m/U_\infty = 0$ the laminar separation point is shifted from $\varphi = 81^\circ$ to higher φ-values, with the separation still remaining laminar, however. Only for higher values of V_m/U_∞, the rotation causes the friction layer to become prematurely turbulent, and it then has the effect of a trip wire whereby a shifting of the critical Reynolds number to lower Reynolds numbers takes place.

Whereas in our theoretical calculations a forward displacement of the separation point occurs, due to the influence of the rotation, the measurements for small values of V_m/U_∞ indicate a shifting of the separation point toward the rear. On the basis of the effect of the centrifugal forces, this must be expected, if one takes into consideration that in the case without rotation the laminar separation point lies, according to theory, behind the equator, according to measurement, however, ahead of the equator. In both cases, the separation point is shifted toward the equator by the effect of the centrifugal forces as is to be expected, at least for small V_m/U_∞, as long as no premature laminar/turbulent transition has been produced by the rotation.

(b) Bodies With a Base (Half-Bodies)

As a second example we shall now treat the so-called half-body (body of revolution I) which originates by superposition of a translational flow on a three-dimensional source flow. If one denotes by R_m the largest radius at infinity, the following parametric representation for the geometrical data of the body[24] is

$$\frac{R}{R_m} = \sin\frac{\varphi}{2} \tag{66}$$

---

[24]For these relationships as well as for the numerical calculations of section 5a, I am indebted to Dr. E. Truckenbrodt. The example calculations of sections 5b and c are taken from the thesis of K. H. Gronau, 1952.

$$\frac{x}{R_m} = \tan\frac{\varphi}{2}\sqrt{1 - \frac{3}{4}\sin^2\frac{\varphi}{2}} + F\left(\frac{\varphi}{2},\sqrt{\frac{3}{4}}\right) - E\left(\frac{\varphi}{2},\sqrt{\frac{3}{4}}\right) \qquad (67)^{25}$$

Here φ is the angle measured from the forward stagnation point. F and E are the incomplete elliptical integrals of the first and second kind for the modulus $\alpha = 60^\circ$.

The velocity distribution is

$$\frac{U}{U_\infty} = 2\sin\frac{\varphi}{2}\sqrt{1 - \frac{3}{4}\sin^2\frac{\varphi}{2}} \qquad (68)$$

The form of the body and the velocity distribution are represented in figure 14. This figure shows, for various values of the spin parameter V_m/U_∞, the variation of the form parameter K with the distance along the body. One sees that already for $V_m/U_\infty \approx 1.3$ only positive values of K result. This means that due to the rotation the laminar friction layer has become more stable because in the present case the centrifugal forces accelerate in the direction of the flow and thus have the effect of an additional pressure drop. We shall forego discussing here all the results. In figure 15 we have represented the torque coefficient $\frac{V_m}{U_\infty}\sqrt{\frac{U_\infty R_m}{\nu}}\,c_M$ against the length L/R_m of the half body. Moreover, the asymptotic solution was drawn in for comparison; one can derive for it the relationship

$$\frac{V_m}{U_\infty}\sqrt{\frac{U_\infty R_m}{\nu}}\,c_M = 8.6\sqrt{\frac{L}{R_m}} \qquad (69)$$

Aside from the torque, the frictional drag also was determined. Figure 16 presents a compilation of the torque coefficient and of the drag coefficient in dependence on the spin parameter V_m/U_∞ for various body lengths L/R_m. It should be emphasized that the drag coefficient is increasing about quadratically with the spin parameter which is in qualitative agreement with the test results that have become known so far.

---

[25] E and F signify

$$F\left(\frac{\varphi}{2},\sqrt{\frac{3}{4}}\right) = \int_0^{\varphi/2}\frac{d\vartheta}{\sqrt{1 - \frac{3}{4}\sin^2\vartheta}} \quad \text{and} \quad E\left(\frac{\varphi}{2},\sqrt{\frac{3}{4}}\right) = \int_0^{\varphi/2}\sqrt{1 - \frac{3}{4}\sin^2\vartheta}\,d\vartheta$$

(c) Streamline Bodies

As further examples we also calculated two streamline bodies of the thickness ratio $D/L = 0.2$ (bodies of revolution II and III). The body shapes and the pertaining velocity distributions were taken from the report of A. D. Young and E. Young[26] (fig. 17). The body of revolution II has as a meridional section a normal profile; the body of revolution III, in contrast, has a laminar profile with the velocity maximum lying relatively far downstream. Of the results, figure 18 shows the torque coefficient and the frictional drag coefficient as a function of the spin parameter V_m/U_∞. In both cases, there are not large differences between the bodies. For the rest, the variation is similar to that in the case of the body with a base. In figure 19, the position of the separation points is shown as a function of the spin parameter V_m/U_∞. In agreement with the values for the rotating sphere (cf. table 4), the separation point shifts forward with increasing rotational speed. This displacement is larger for the body of revolution II than for the body of revolution III which is made understandable by the position of the velocity maximum. Finally, we gave for the body of revolution II a graphic representation of the velocity distributions in the friction layer for the spin parameters $V_m/U_\infty = 0$ and $V_m/U_\infty = 1$ (fig. 20). From it one sees that ahead of the pressure minimum the meridional velocity component does not vary noticeably due to the influence of the rotation whereas between the pressure minimum and the separation point the influence of the rotation is considerable.

6. SUMMARY

A calculation method is given by which the flow about a rotating body of revolution in a flow which approaches in the direction of the axis of rotation may be determined on the basis of boundary-layer theory. The investigations yield a contribution to the aerodynamics of a projectile with spin. The calculation is carried out for the laminar boundary layer with the aid of the momentum theorem which is stated for the meridional and for the circumferential direction. The performance of the calculation requires the solution of two ordinary simultaneous differential equations of the first order. It yields, in addition to the boundary-layer parameters, the frictional drag and the torque as a function of the dimensionless spin coefficient V_m/U_∞ = circumferential velocity/free-stream velocity. The displacement of the separation point

---

[26] A. D. Young, E. Young, "A family of streamline bodies of revolution suitable for high-speed and low-drag requirements." ARC Report 2204, 1951.

with the spin coefficient also is obtained. As examples, the flow about a rotating sphere, about a body with a base, and about two streamline bodies is treated.

Translated by Mary L. Mahler
National Advisory Committee
for Aeronautics

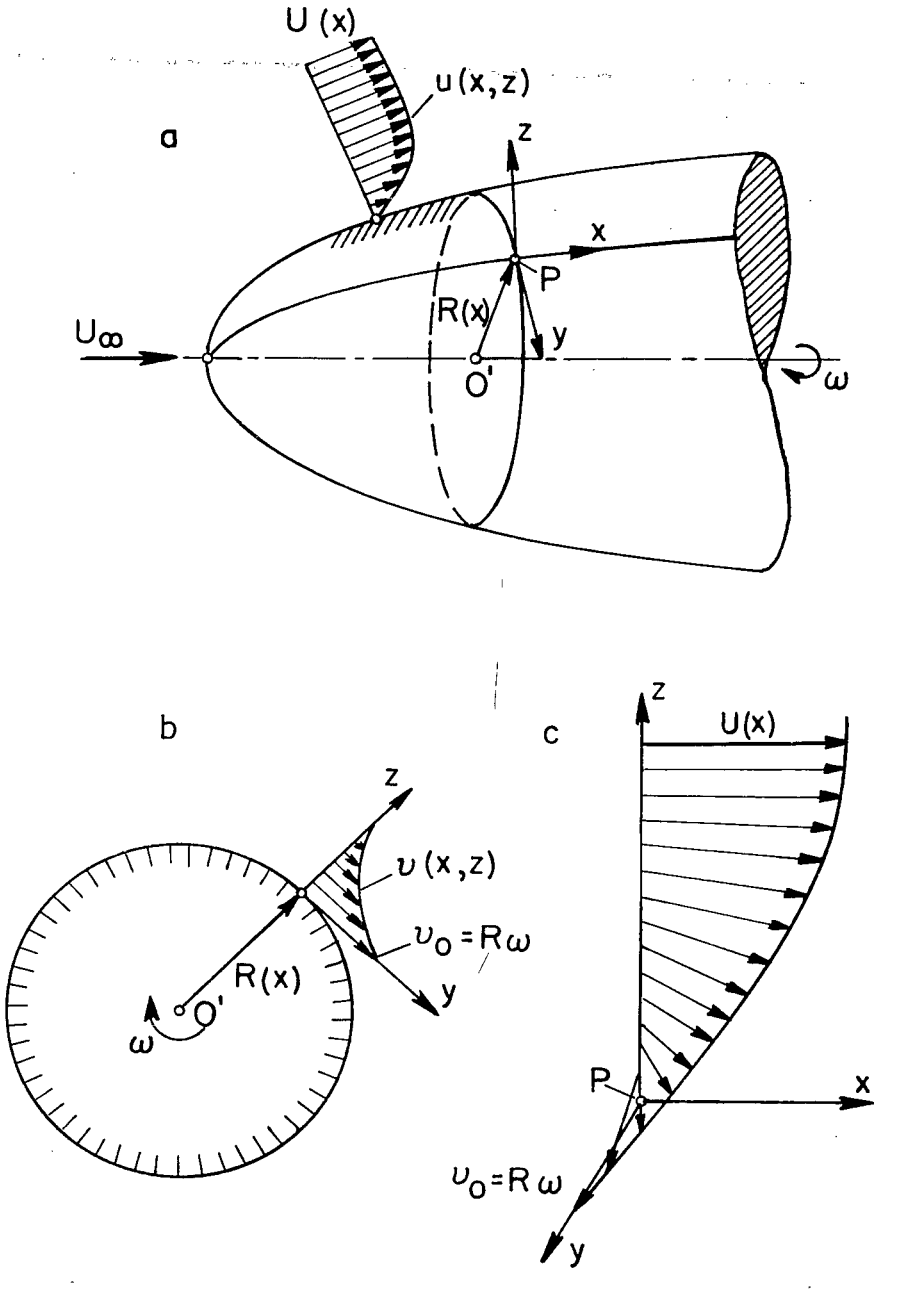

Figure 1.- Explanatory sketch.

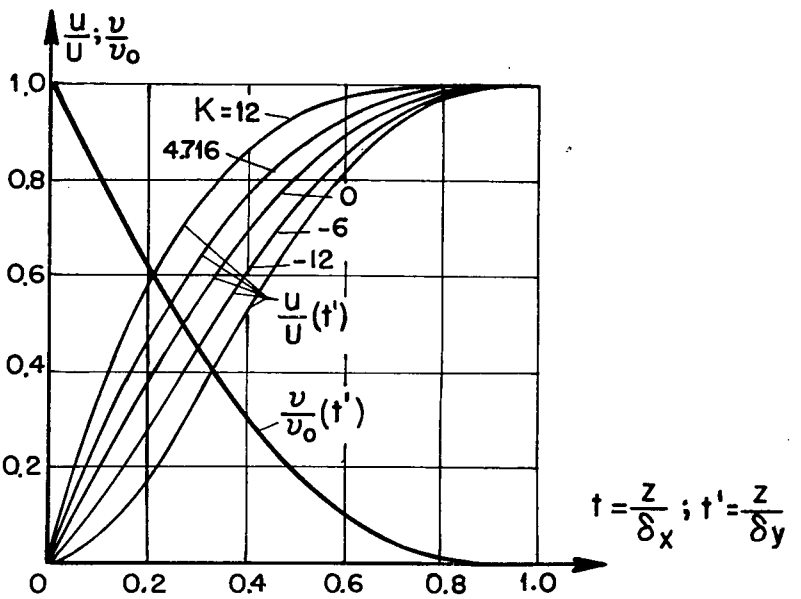

Figure 2.- Velocity distributions in meridional and in azimuthal direction.

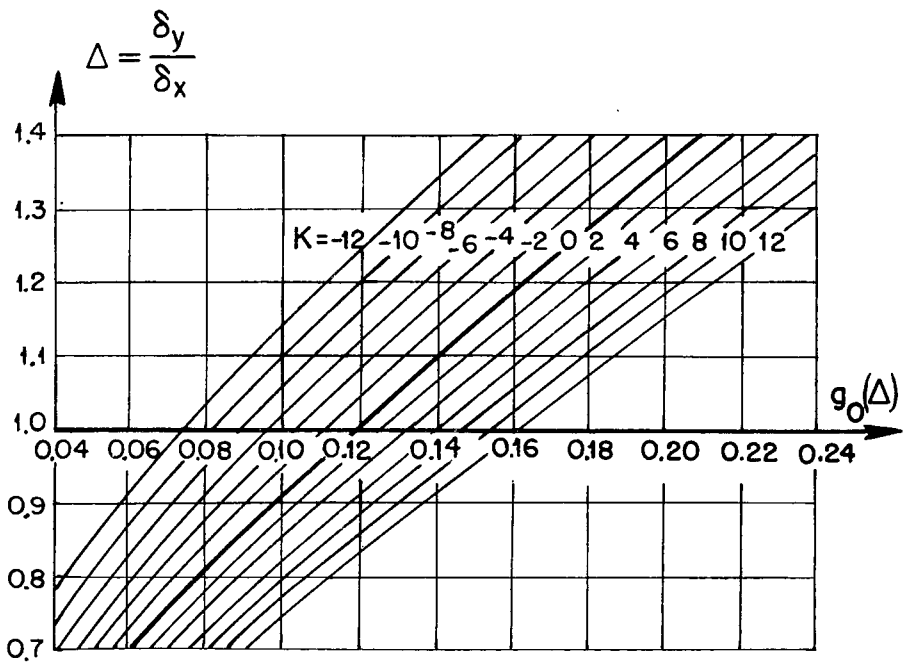

Figure 3.- The universal function $\Delta = \delta_y/\delta_x$ as a function of $g_0(\Delta) = \delta_{xy}/\delta_x$ according to (27) and (28).

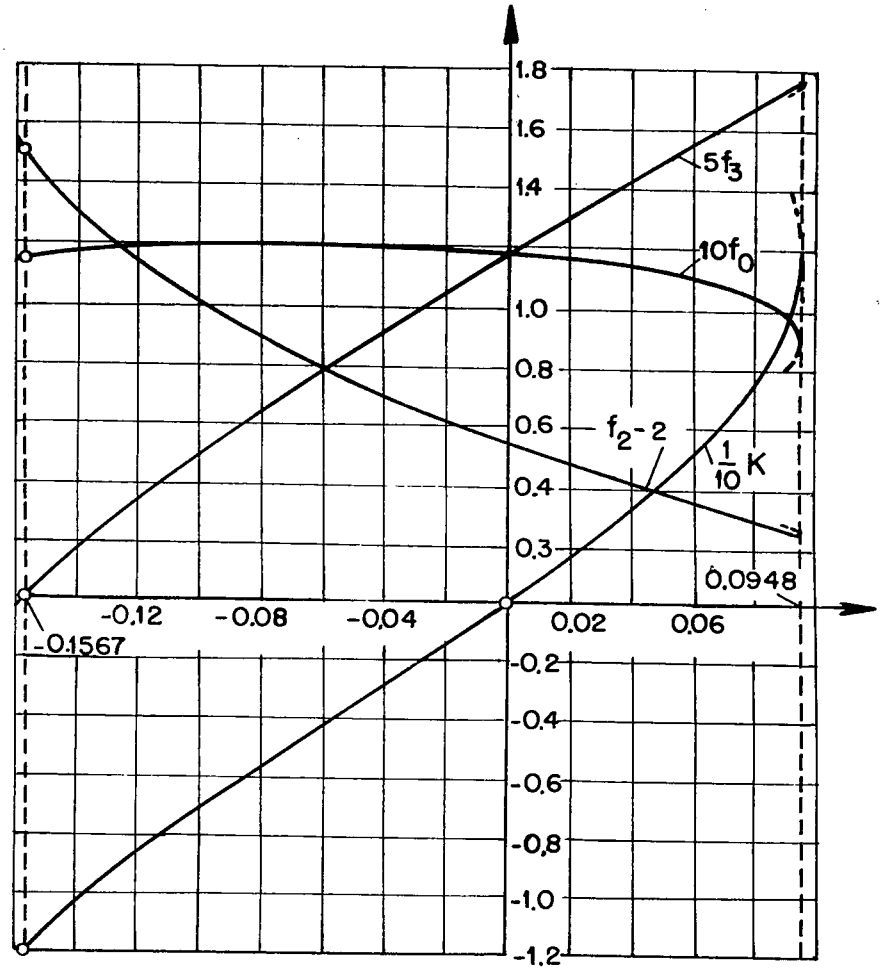

Figure 4.- The universal functions $f_0 = \vartheta_x/\delta_x$, $f_2 = \delta_x^*/\vartheta_x$, $f_3 = \tau_{x0}/\mu\ \vartheta_x/U$ and K as a function of x^* according to (32) to (39).

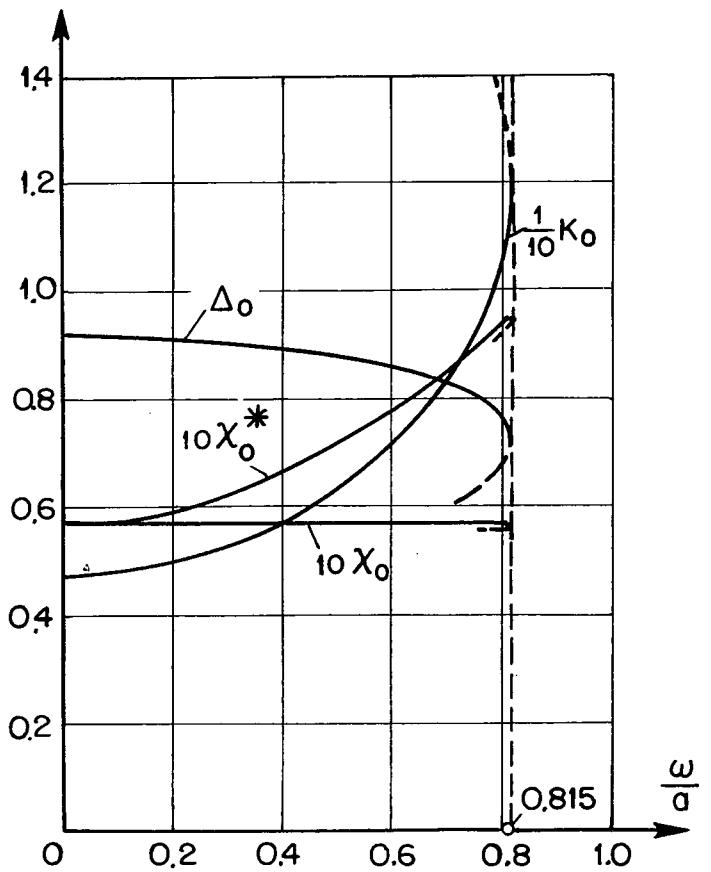

Figure 5.- The initial values at the stagnation point Δ_0, K_0, χ_0, and χ_0^*.

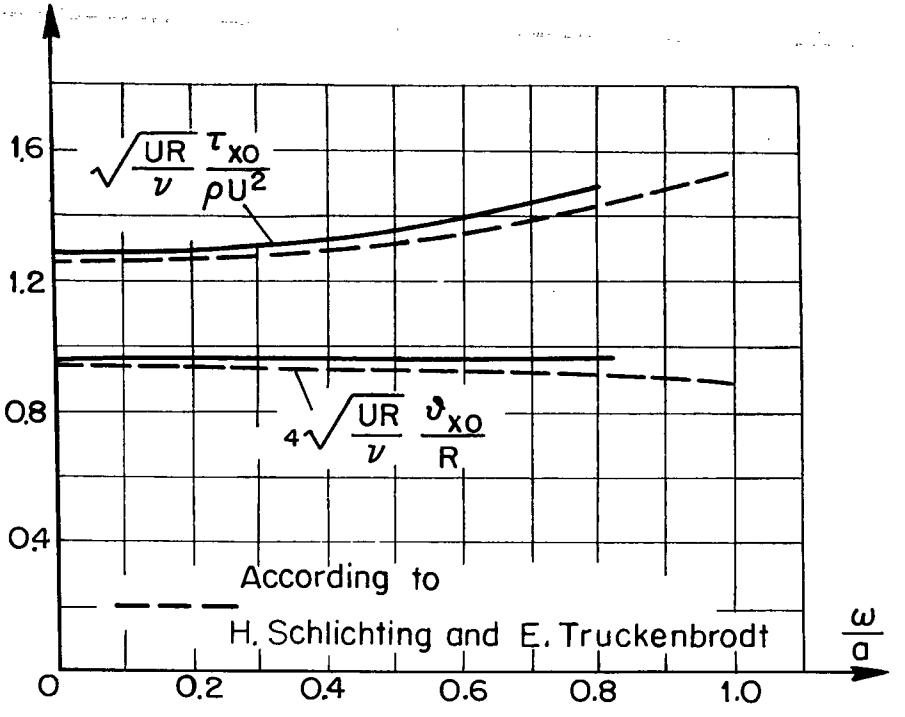

Figure 6.- Momentum-loss thickness ϑ_x and wall-shear stress τ_{x0} at the stagnation point. Comparison with the values of the rotating disk in a flow according to H. Schlichting and E. Truckenbrodt.

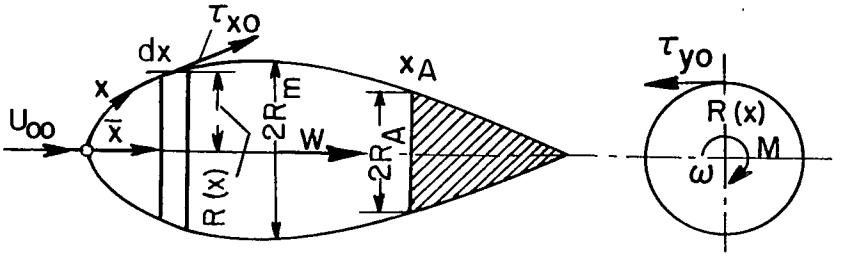

Figure 7.- Sketch for calculation of the torque and of the frictional drag.

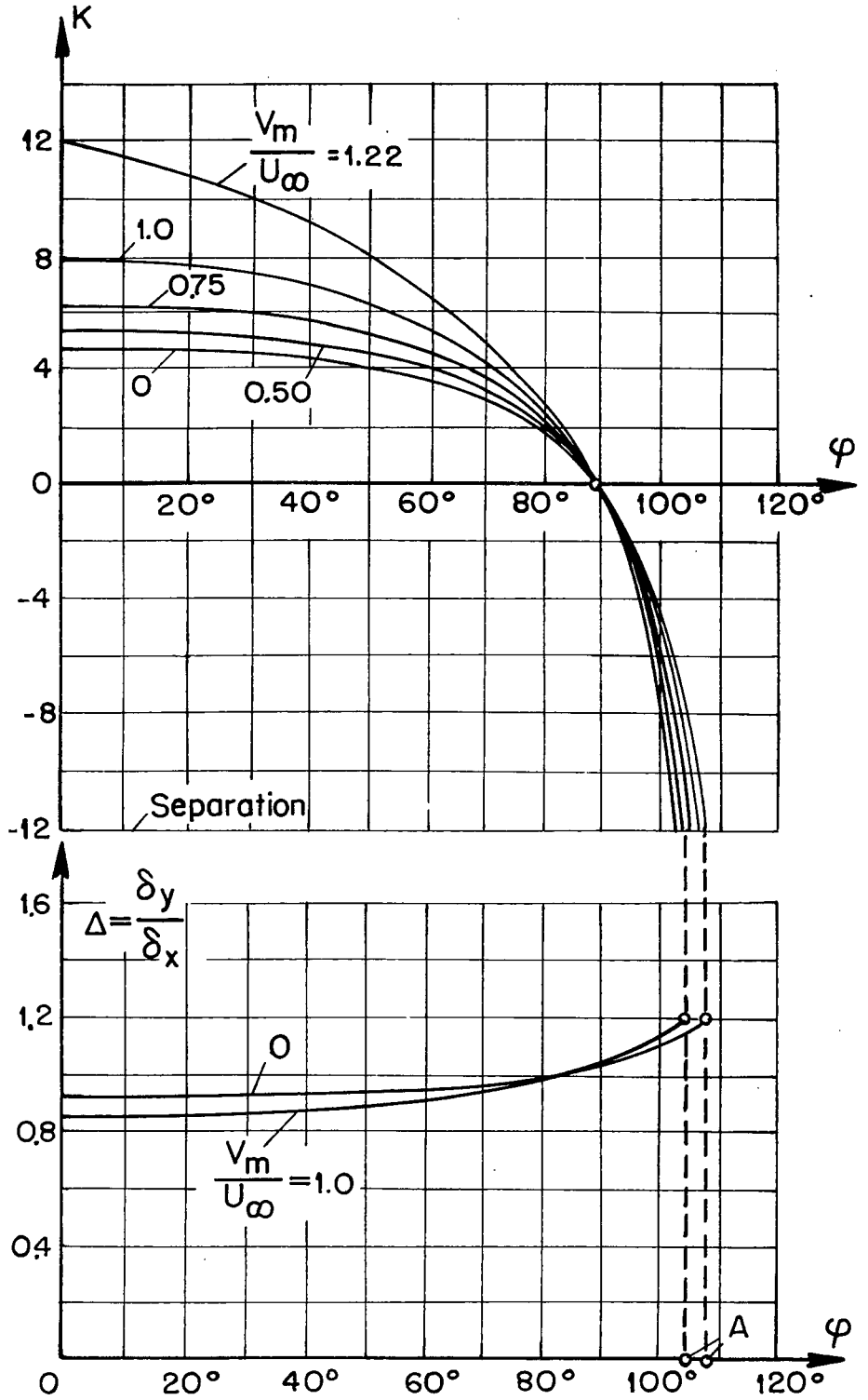

Figure 8.- Form parameter K and boundary-layer thickness ratio $\Delta = \delta_y/\delta_x$ for the rotating sphere in a flow for different spin parameters V_m/U_∞.

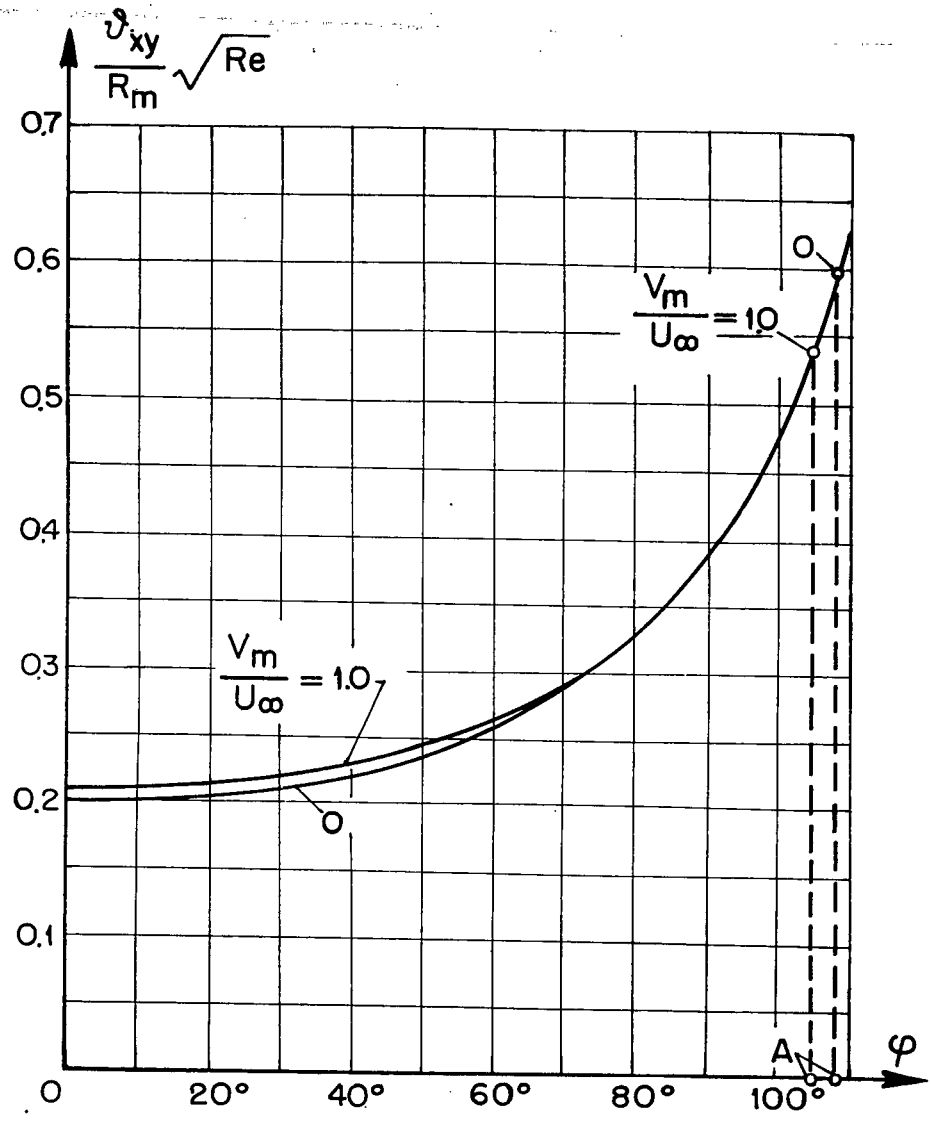

Figure 9.- Momentum-loss thickness due to spin ϑ_{xy} for the rotating sphere in a flow. $Re = U_\infty R_m/\nu$.

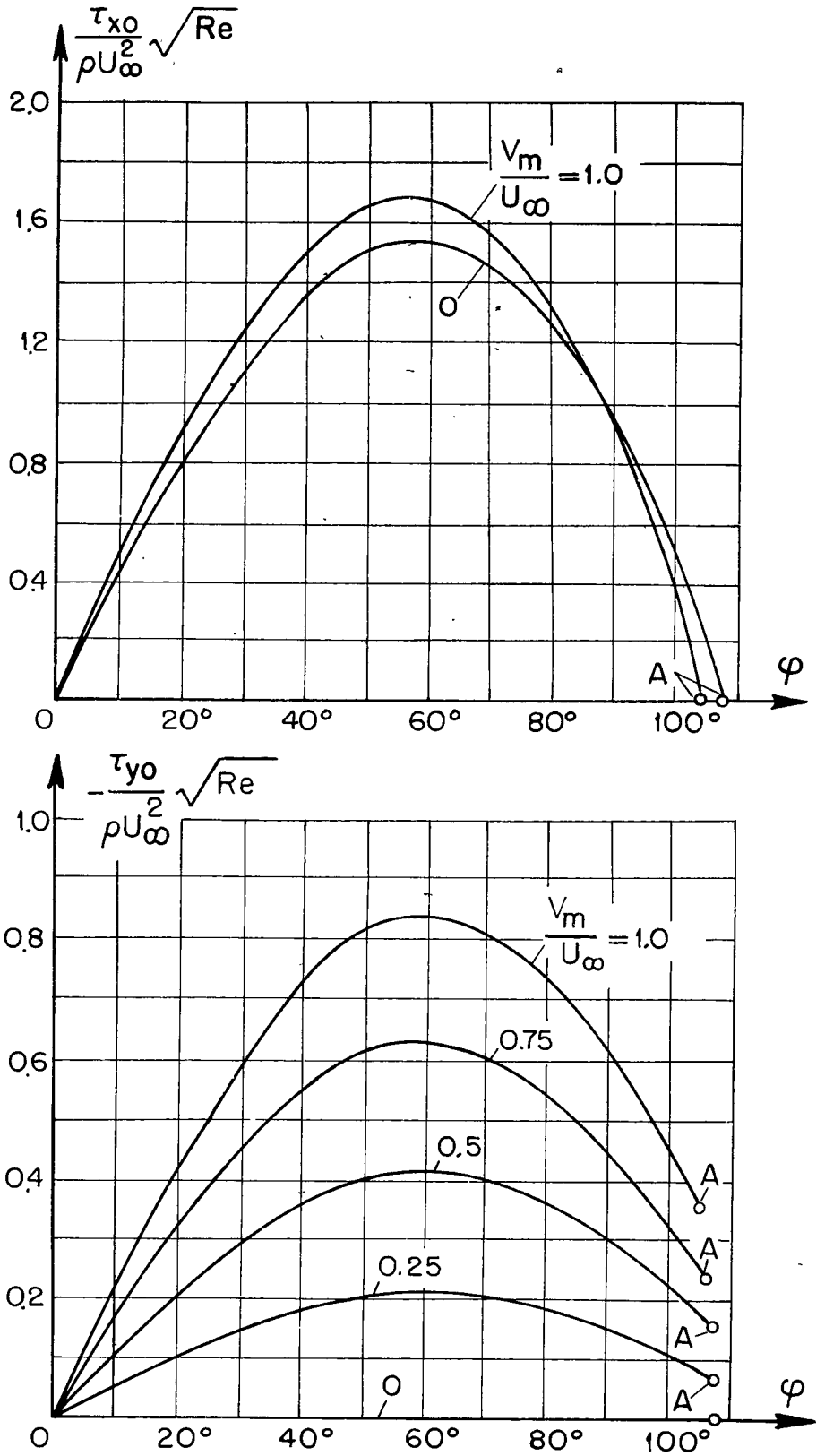

Figure 10.- The wall-shear stress components in meridional and azimuthal direction τ_{x0} and τ_{y0} for the rotating sphere in a flow. $Re = U_\infty R_m/\nu$.

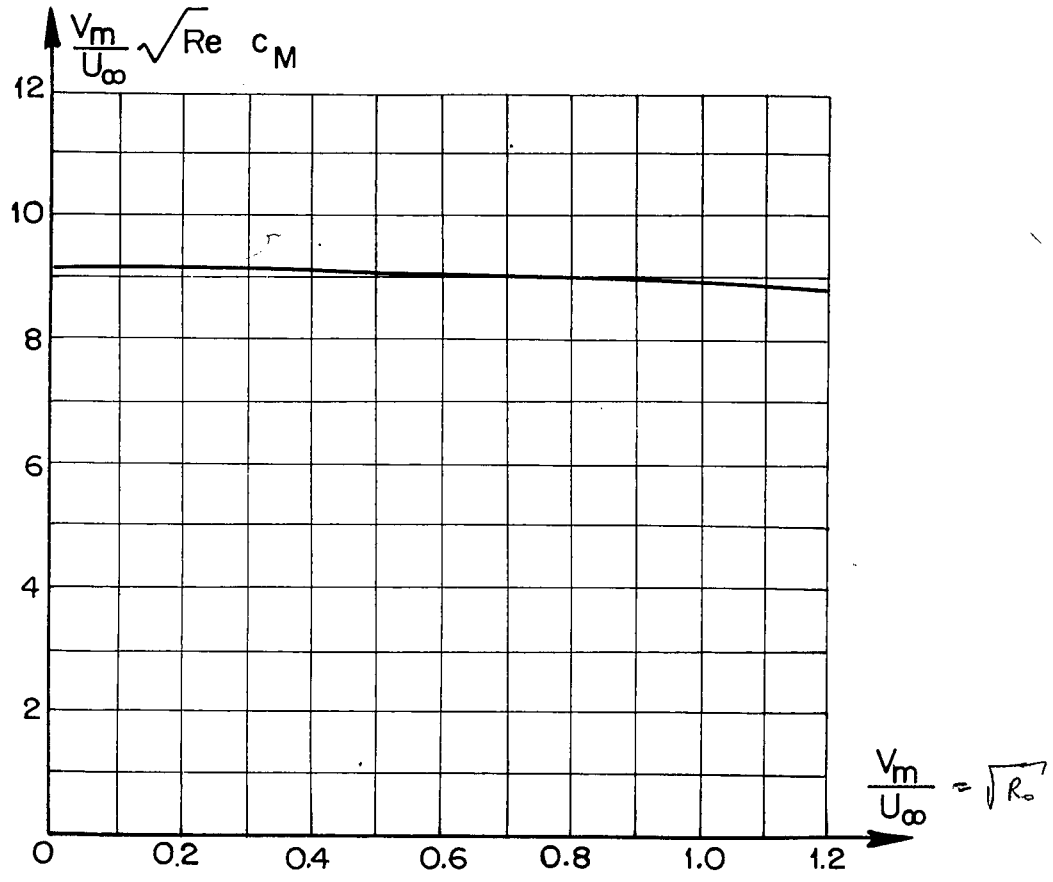

Figure 11.- Torque coefficient c_M for the rotating sphere in a flow. $Re = U_\infty R_m/\nu$.

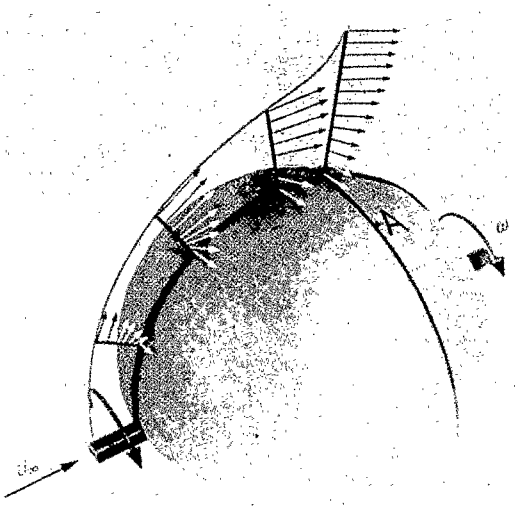

Figure 12.- Photographic representation of the velocity distributions in the boundary layer of the rotating sphere in a flow, $V_m/U_\infty = 1$, A = separation line.

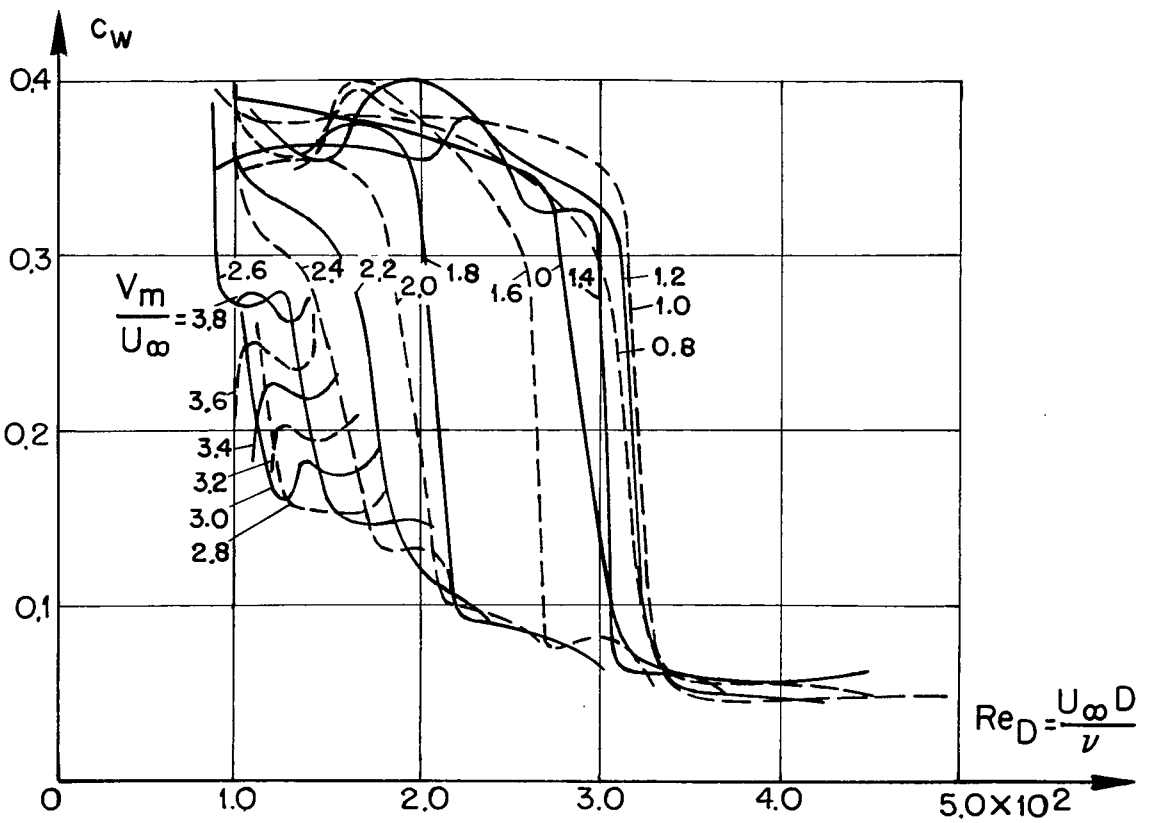

Figure 13.- Drag coefficients of the rotating sphere in a flow as a function of the Reynolds number, according to measurements of S. Luthander and A. Rydberg.

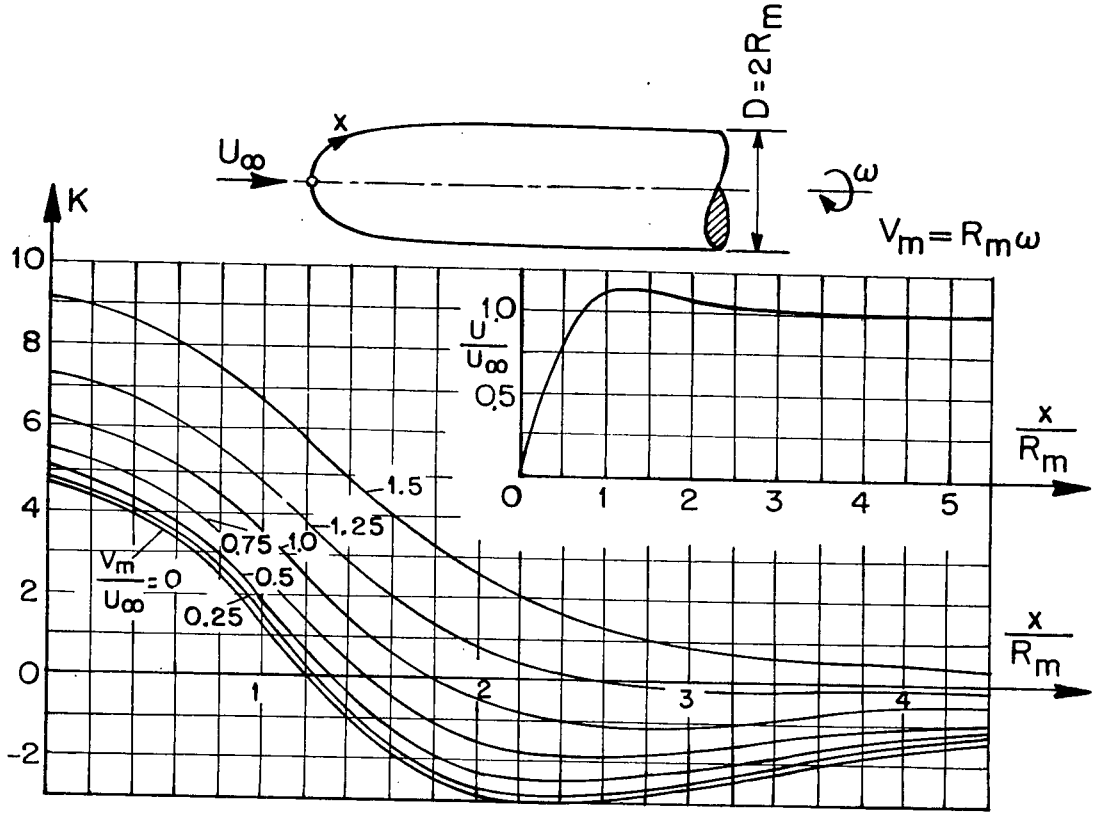

Figure 14.- Form parameter K for the rotating body with a base in a flow (body of revolution I).

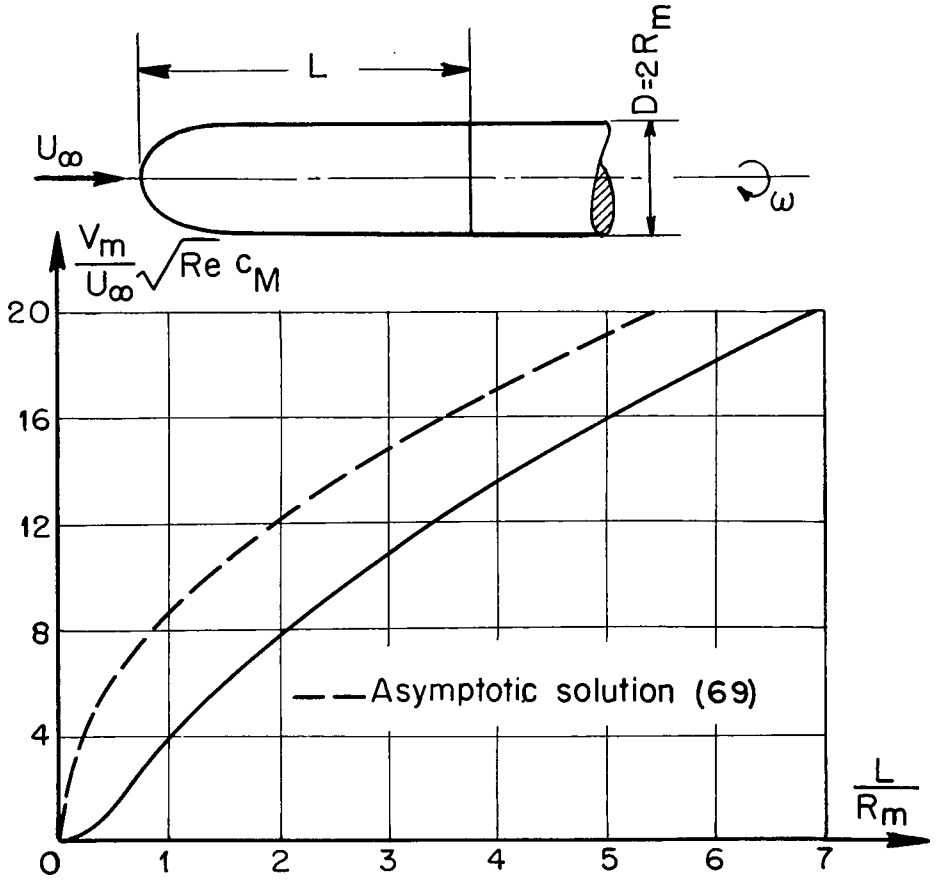

Figure 15.- Torque coefficient c_M for the rotating body with a base in a flow as a function of the length of the body. $Re = U_\infty R_m/\nu$.

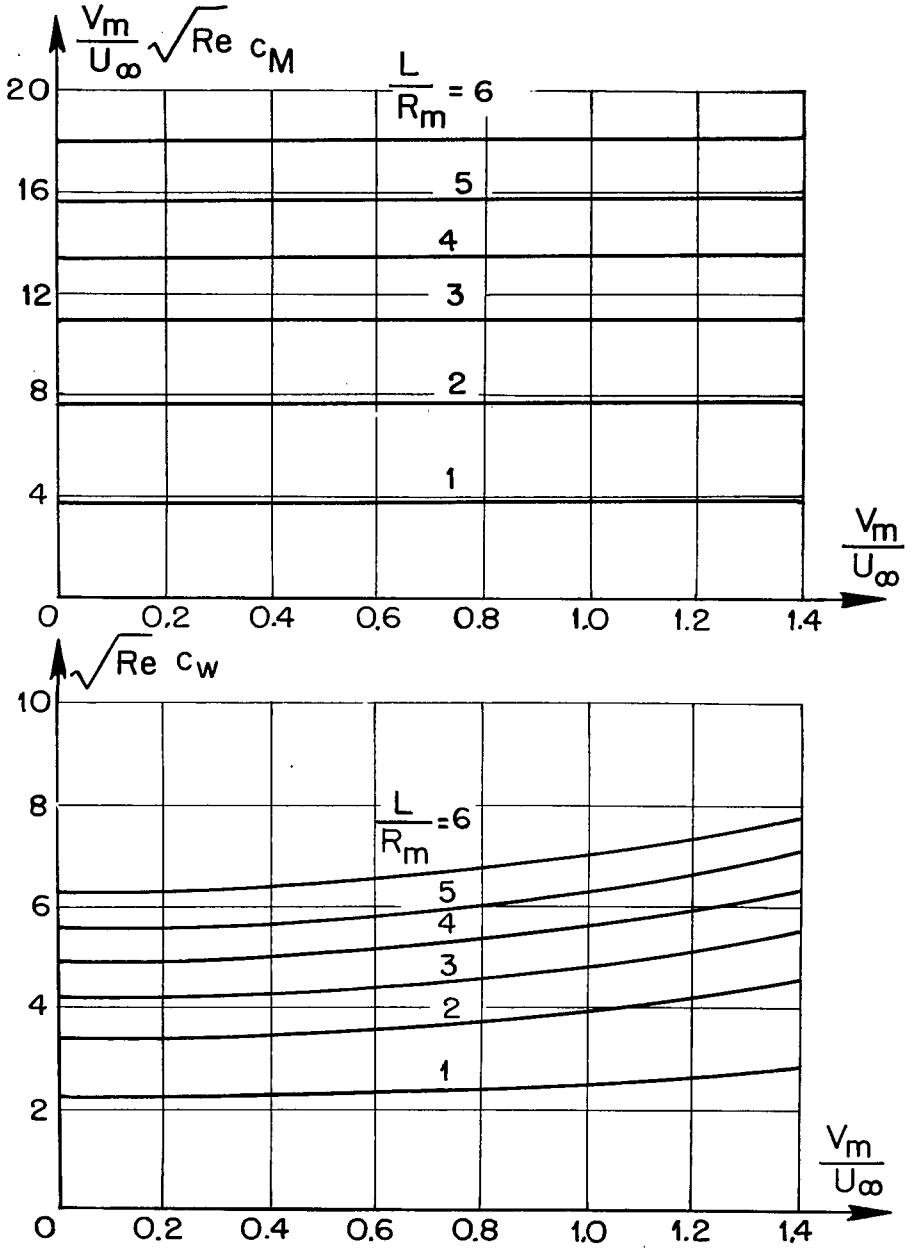

Figure 16.- Torque coefficient c_M and drag coefficient c_W for the rotating body with a base in a flow (body of revolution I) as a function of the spin parameter V_m/U_∞. $Re = U_\infty R_m/\nu$.

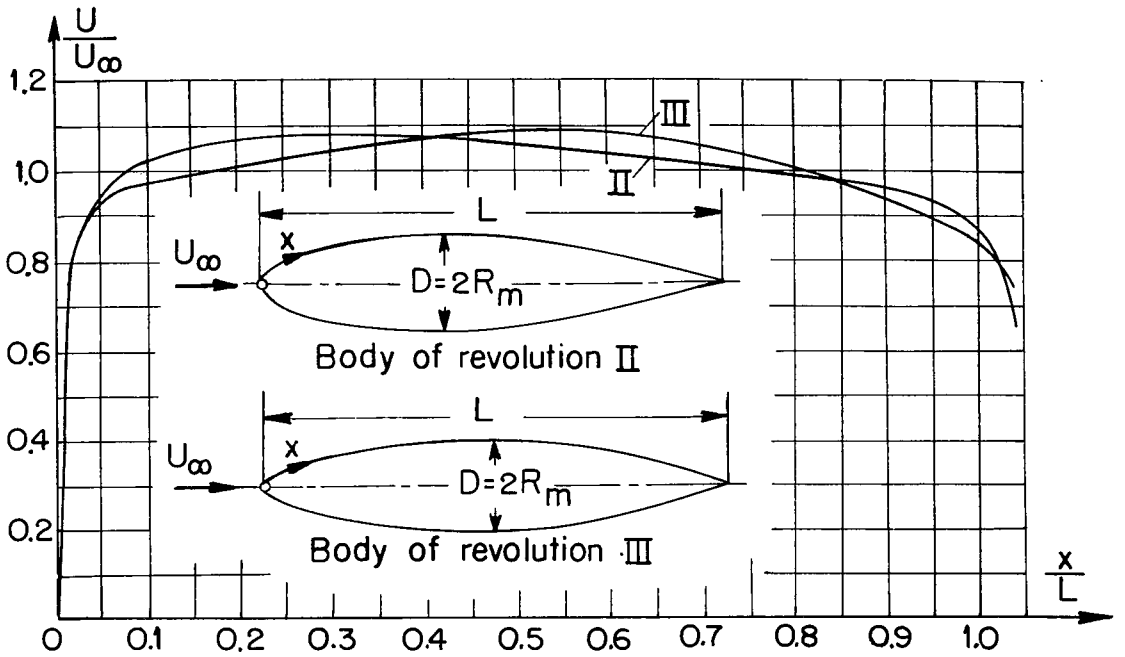

Figure 17.- Body shape and potential flow for two streamline bodies (bodies of revolution II and III); D/L = 0.2.

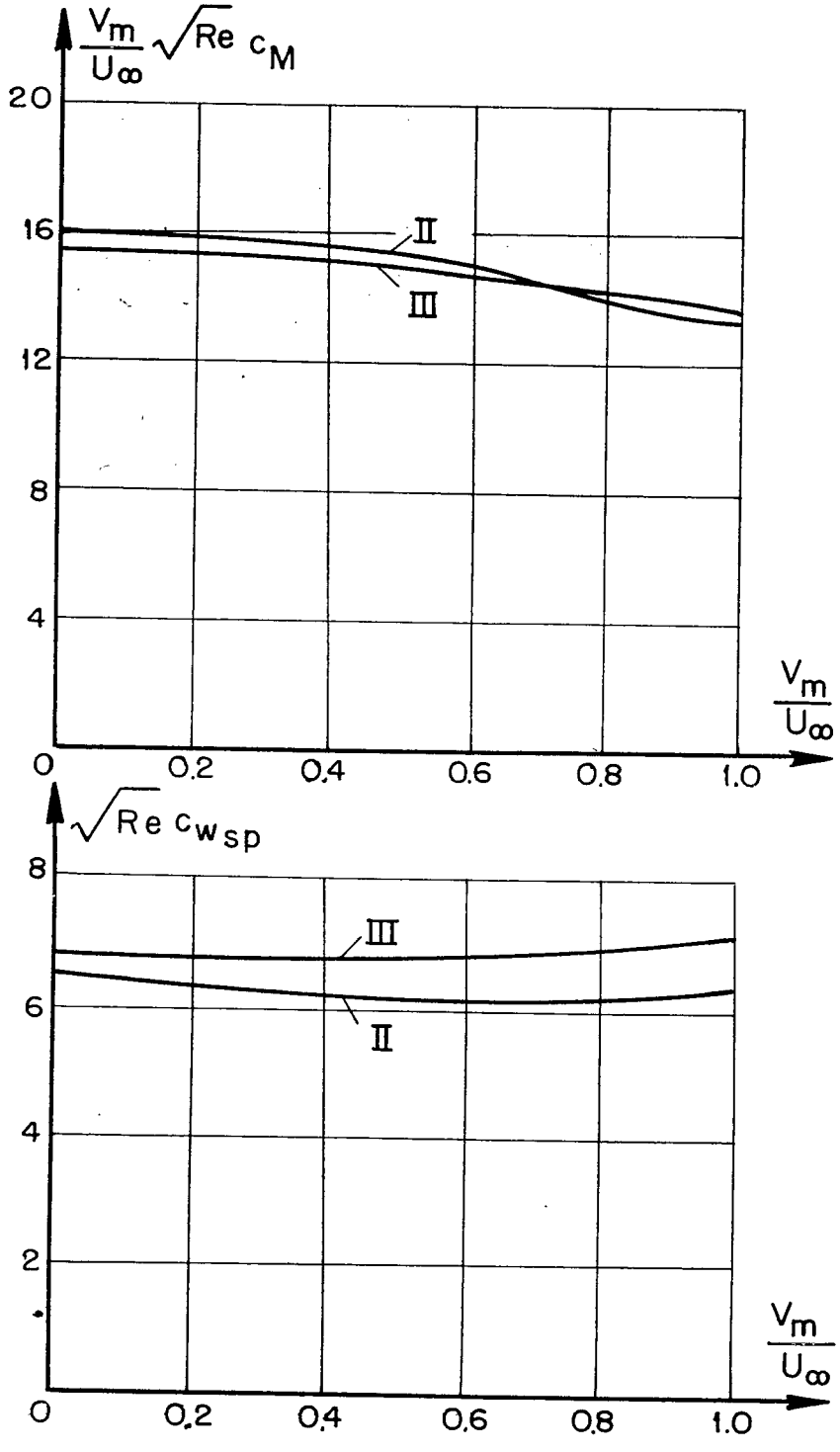

Figure 18.- Torque coefficient c_M and drag coefficient c_w for the two streamline bodies according to figure 17 as a function of the spin parameter V_m/U_∞. $Re = U_\infty R_m/\nu$.

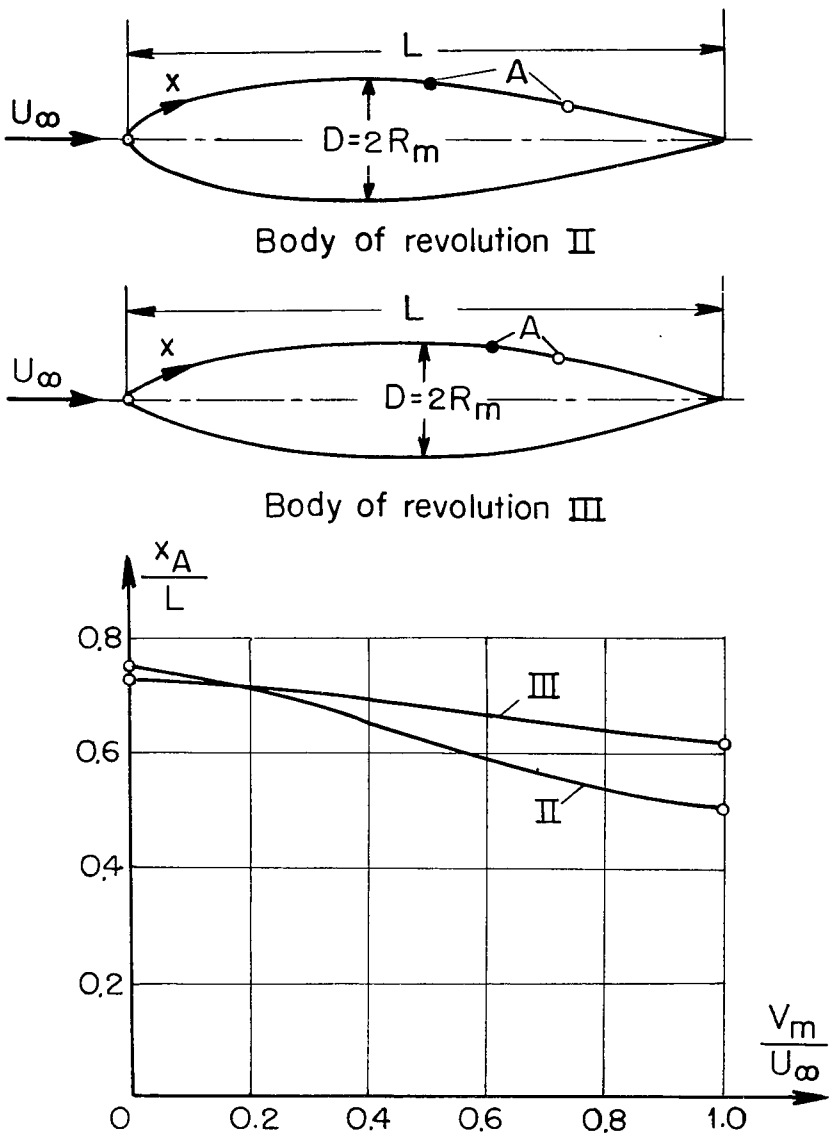

Figure 19.- Position of the separation point A for the two streamline bodies according to figure 17 as a function of the spin parameter V_m/U_∞. Position of the separation point: o for $V_m/U_\infty = 0$; ● for $V_m/U_\infty = 1$.

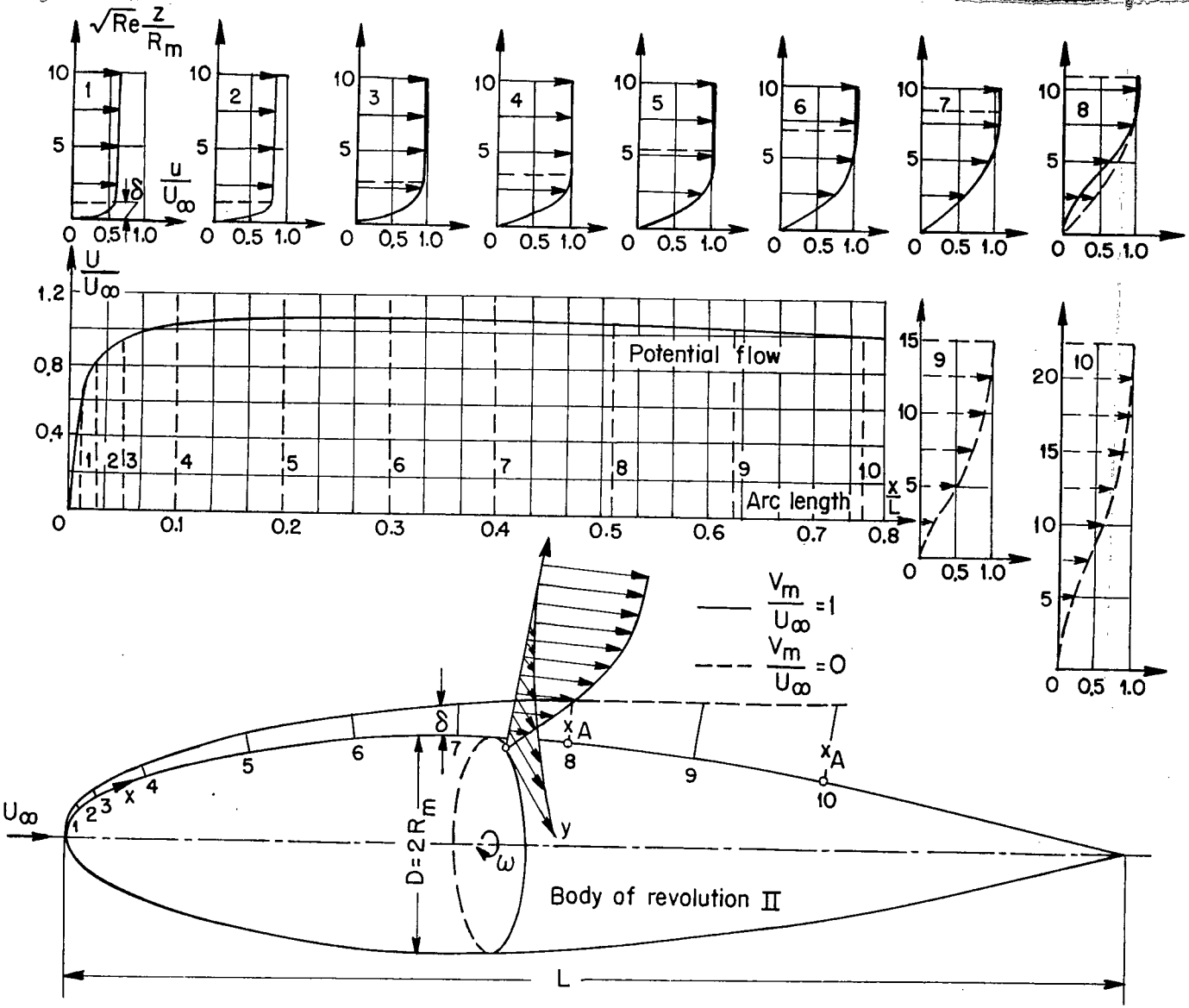

Figure 20.- Velocity distribution in the boundary layer on the body of revolution II for the spin parameters $V_m/U_\infty = 0$ and $V_m/U_\infty = 1.0$. $Re = U_\infty R_m/\nu$. In the lower figure the boundary-layer thickness δ is magnified $1/30\sqrt{Re}$-fold.